ACC03-ASME0018

Controller Design for Flexible Systems with Friction: Linear Programming Approach

Jae-Jun Kim
jjk@eng.buffalo.edu
Tarunraj Singh
tsingh@eng.buffalo.edu
State University of New York at Buffalo, Buffalo, NY 14260

Abstract

The design of a controller for a flexible system under the influence of friction is presented. A linear programming technique for finding an optimal control of linear flexible systems is extended to frictional systems. A floating oscillator is used in the development, where friction and control input forces are acting on the first mass. The result of the linear programming is a control profile for rest-to-rest maneuvers where the static and Coulomb friction is included in the system model. The positive pulse controller is also developed based on the available frictional force. These controllers can be applied to precision positioning systems and servo applications where the friction and flexibility are significant.

1 Introduction

Friction is the most commonly encountered nonlinearities in mechanical systems. Various compensation techniques are available for regulating problems such as adaptive friction feedforward/feedback and impulsive control [1],[2]. The stick-slip effect is accentuated for regulating flexible systems at the small velocity region and velocity reversals. One way of keeping the system stick-slip free is to maintain positive velocity of the frictional body during the maneuver. This positive velocity assumption of the frictional body creates a constant Coulomb friction, which is a bias force term added to the input force. From this assumption, optimal control techniques for linear systems can be used to design a controller. One method to design a controller for linear system is a frequency domain approach, where time delay filters are used to obtain the time optimal controller [3]. However, prior knowledge of bang-bang control profile for linear systems is not valid because of the constraints imposed on the first mass velocity. Another approach to solve this problem is linear programming [4]. Although the accuracy of the control profile is limited by the number of samples and convergence tolerance, linear programming guarantees to generate a globally optimal control profile. A floating oscillator with a friction model used in the controller design can represent many applications such as hard disk drives and flexible robots where friction is present at the actuator and the end effector position needs to be regulated.

2 Floating Oscillator with Friction

A floating oscillator under the influence of friction is shown in Figure 2. The equation of motion of the system can be written as

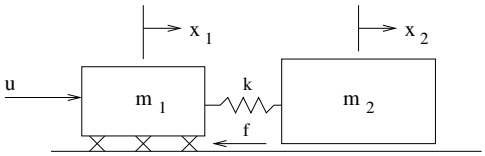

Figure 1: Floating Oscillator under Friction

$$\dot{\underline{x}}(t) = A\underline{x}(t) + Bu(t) - Bf(\underline{x}, u) \tag{1}$$

where, state vector $\underline{x} = [x_1 \quad x_2 \quad \dot{x}_1 \quad \dot{x}_2]^T$, u is a control input, f is a friction force, and

$$A = \begin{bmatrix} 0 & 0 & 1 & 0 \\ 0 & 0 & 0 & 1 \\ -\frac{k}{m_1} & \frac{k}{m_1} & 0 & 0 \\ \frac{k}{m_2} & -\frac{k}{m_2} & 0 & 0 \end{bmatrix} \quad B = \begin{bmatrix} 0 \\ 0 \\ \frac{1}{m_1} \\ 0 \end{bmatrix} \tag{2}$$

Static and Coulomb friction model is used in the development, and the friction force f is defined as

$$f = \begin{cases} f_c sgn(\dot{x}_1) & \text{if } \dot{x}_1 \neq 0 \\ f_s sgn(u_s) & \text{if } \dot{x}_1 = 0 \text{ and } u_s > f_s \\ u_s & \text{if } \dot{x}_1 = 0 \text{ and } u_s \leq f_s \end{cases} \tag{3}$$

where, f_c is coulomb friction and f_s is static friction. u_s is the sum of control input and spring force applied to the first mass, which is

$$u_s = u + k(x_2 - x_1) \tag{4}$$

3 Linear Programming Formulation

The system model can be linearized if the velocity of the first mass is always positive. With this assumption,

the friction force becomes

$$f = f_c \qquad (\text{if } \dot{x}_1 > 0) \tag{5}$$

In discrete time, the system equation is written as

$$\underline{x}_{k+1} = A_d \underline{x}_k + B_d(u_k - f_c) \tag{6}$$

where, $k = 1, 2, ..., N$. The initial and final states are given as

$$\underline{x}_1 = \underline{x}(0), \quad \underline{x}_{N+1} = \underline{x}(t_f) \tag{7}$$

Where, t_f is the total maneuver time. The linear programming problem is to find a minimum t_f while satisfying system equation with initial/final state constraints, velocity constraints and input constraints, which is similar to the approach in [4]. The state vector at the final time can be computed from the initial condition and control history such that

$$\underline{x}_{N+1} = A_d^N \underline{x}_1 + \sum_{i=1}^{N} A_d^{N-i} B_d u_i - \sum_{i=1}^{N} A_d^{N-i} B_d f_c \tag{8}$$

By rewriting Equation 8, the equality constraints on the final states becomes

$$\begin{bmatrix} A_d^{N-1}B_d & A_d^{N-2}B_d & \cdots & A_dB_d & B_d \end{bmatrix} \begin{bmatrix} u_1 \\ u_2 \\ \cdot \\ \cdot \\ \cdot \\ u_N \end{bmatrix}$$

$$= \underline{x}_{N+1} - A_d^N \underline{x}_1 + \sum_{i=1}^{N} A_d^{N-i} B_d f_c \tag{9}$$

Assumption of the positive velocity for the first mass leads to inequality constraints. Define a output vector $C_d = [0 \quad 0 \quad 1 \quad 0]^T$, the velocity of the first mass becomes

$$\dot{x}_{1,k+1} = C_d A_d^k \underline{x}_1 + \sum_{i=1}^{k} C_d A_d^{k-i} B_d u_i - \sum_{i=1}^{k} C_d A_d^{k-i} B_d f_c \tag{10}$$

where, $k = 1, 2, \cdots, N$. Because of the positive velocity assumption of the first mass, we arrive at the constraint

$$\dot{x}_{1,k+1} > 0 \qquad (k = 1, 2, \cdots, N-1) \tag{11}$$

In order to form a standard linear programming problem, the above equation can be written as

$$\dot{x}_{1,k+1} \geq \epsilon \qquad (k = 1, 2, \cdots, N-1) \tag{12}$$

where, ϵ is a small positive number.

Another constraints to the design is that the first input should be greater than the static friction in order to start the maneuver. That is

$$u_1 \geq f_s + \epsilon \tag{13}$$

Inequality constraint in Equation 12 and 13 can be represented in a matrix form as

$$\begin{bmatrix} -1 & 0 & \cdots & 0 \\ -C_dB_d & 0 & \cdots & 0 \\ -C_dA_dB_d & -C_dB_d & \cdots & 0 \\ \cdot & \cdot & & \cdot \\ \cdot & & \cdot & \cdot \\ \cdot & & & \cdot \\ -C_dA_d^{N-2}B_d & -C_dA_d^{N-3}B_d & \cdots & -C_dB_d \end{bmatrix} \begin{bmatrix} u_1 \\ u_2 \\ u_3 \\ \cdot \\ \cdot \\ \cdot \\ u_N \end{bmatrix}$$

$$\leq \begin{bmatrix} -f_s - \epsilon \\ C_dA_d\underline{x}_1 - C_dB_df_c - \epsilon \\ C_dA_d^2\underline{x}_1 - C_dA_dB_df_c - C_dB_df_c - \epsilon \\ \cdot \\ \cdot \\ \cdot \\ C_dA_d^{N-1}\underline{x}_1 - \sum_{i=1}^{N-1} C_dA_d^{N-1-i}B_df_c - \epsilon \end{bmatrix} \tag{14}$$

The control input has lower and upper bounds such that

$$-u_p \leq u_k \leq u_p \qquad (k = 1, 2, \cdots, N) \tag{15}$$

where, u_p is a maximum control input value.

4 Numerical Simulation

Numerical simulation was performed using `Matlab`. The parameter values used in the simulation are shown in Table 1. The first simulation is performed with the

Table 1: Parameters Used in the Simulation

m_1	80 Kg
m_2	100 Kg
k	111111.1111 Kg/sec^2
u_p	500 N
f_s	137 N
f_c	111 N

initial and final states of

$$\underline{x}(0) = \begin{bmatrix} 0 \\ 0 \\ 0 \\ 0 \end{bmatrix} \qquad \underline{x}(t_f) = \begin{bmatrix} 0.1 \\ 0.1 \\ 0 \\ 0 \end{bmatrix} \tag{16}$$

The control input history and its discrete time linear simulation response are shown in Figure 2 and 3 for the above initial and final states. The velocity of the first mass plotted with solid line in Figure 3 remains positive during the maneuver. Corresponding input is a bang-bang profile with three switches.

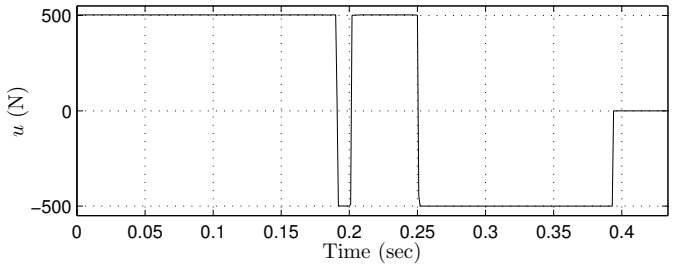

Figure 2: Input Force, displacement 0.1 m

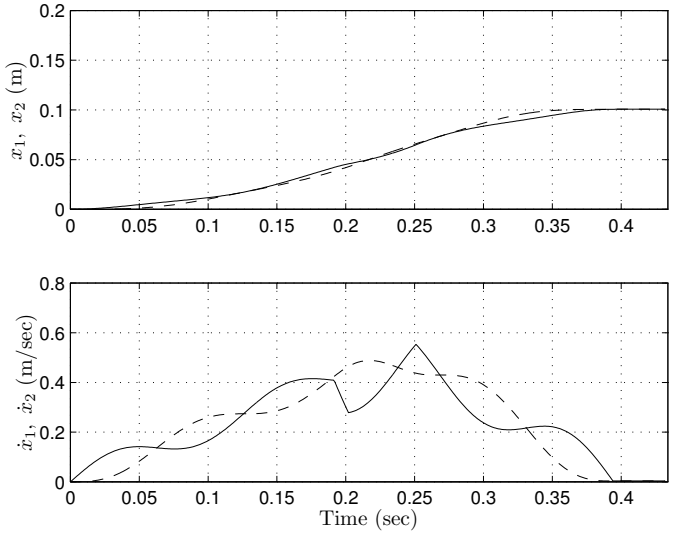

Figure 3: Response Plot, displacement 0.1 m

The second simulation is performed with the initial and final states of

$$\underline{x}(0) = \begin{bmatrix} 0 \\ 0 \\ 0 \\ 0 \end{bmatrix} \qquad \underline{x}(t_f) = \begin{bmatrix} 0.001 \\ 0.001 \\ 0 \\ 0 \end{bmatrix} \tag{17}$$

The corresponding control input history and its response are shown in Figure 4 and 5. The response plot in Figure 5 shows that the velocity of the first mass stays very close to zero during the maneuver for some time. In fact, the velocity of the first mass stays zero for some time if ϵ in Equation 12 approaches to zero.

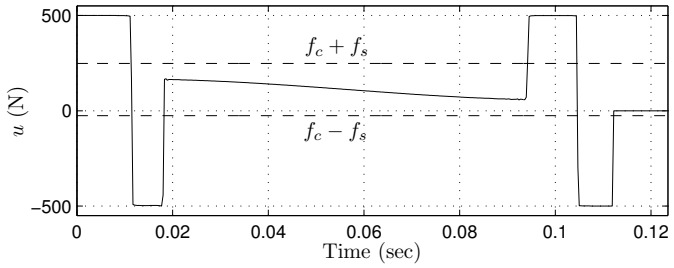

Figure 4: Input Force, displacement 0.001 m

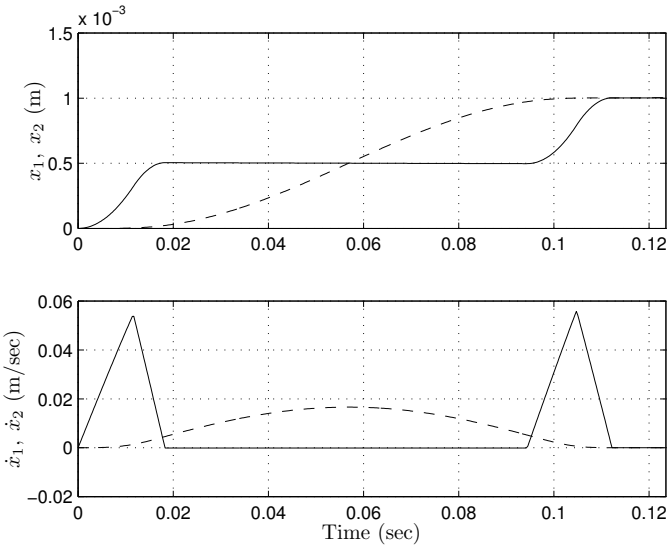

Figure 5: Response Plot, displacement 0.001 m

In Figure 4, the controller is trying to compensate the Coulomb friction and spring force in order to maintain stiction of the first mass. However, Coulomb friction force disappears when the first mass is sticking. Therefore, the controller doesn't need to compensate Coulomb friction when the first mass velocity is zero. In addition, if the spring force is not enough to overcome static friction, the first mass will stay stuck. This condition leads to an equivalent control, u_{eq}, as

$$u_{eq,k} = 0 \quad \text{if } f_c - f_s < u_k < f_c + f_s \text{ and } \dot{x}_{1,k} = 0 \tag{18}$$

where, $k = 1, 2, \cdots, N$. Therefore, the equivalent control profile to Figure 4 becomes bang off bang as shown in Figure 6.

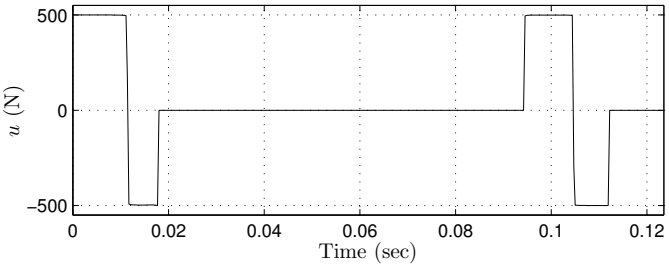

Figure 6: Equivalent Input Force, $d = 0.001$ m

The third simulation is with the initial and final condition of

$$\underline{x}(0) = \begin{bmatrix} 0 \\ 0 \\ 0 \\ 0 \end{bmatrix} \qquad \underline{x}(t_f) = \begin{bmatrix} 0.01 \\ 0.01 \\ 0 \\ 0 \end{bmatrix} \tag{19}$$

With these conditions, the input history and corre-

sponding response plots are shown in Figure 7 and Figure 8.

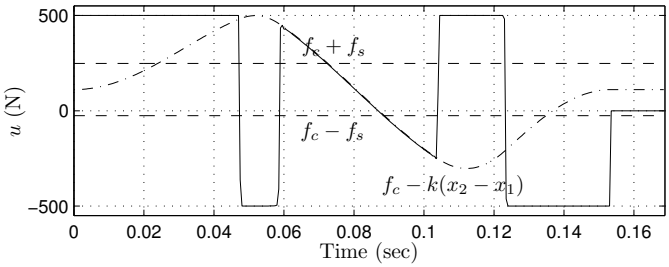

Figure 7: Input Force, displacement 0.01 m

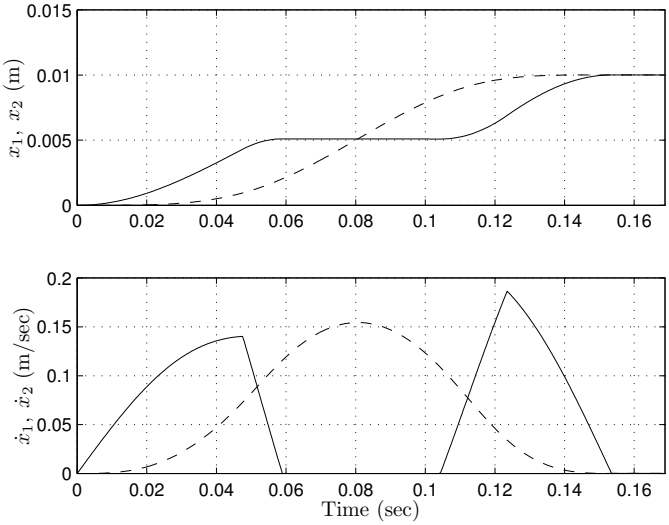

Figure 8: Response Plot, displacement 0.01 m

Input profile shown in Figure 7 shows that the compensation force to maintain the stiction of the first mass coincide with the plot of $f_c - k(x_2 - x_1)$. However, the input during stiction is not always within the upper and lower bounds. Because the Coulomb friction disappears during stiction, only spring force is needed to be compensated to stay stuck. Therefore, Coulomb friction is subtracted from the input profile during the stiction and the equivalent input profile is shown in Figure 9. It is also possible to turn off the controller when the input is within the bounds (Equation 18), however, turning off the controller near the bounds may result in the movement of the first mass when there is a slight variation of the static friction value.

5 Positive Pulse Approach

For a floating oscillator without friction, controller must have a negative input in order to bring the system to a stop. However, controller for a floating oscillator

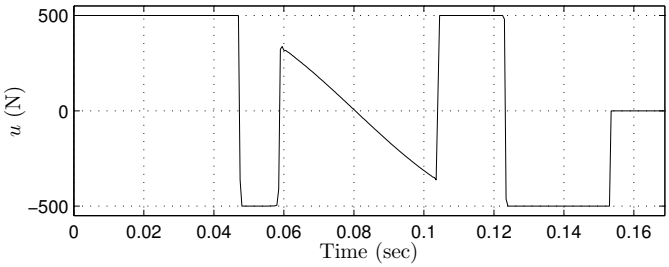

Figure 9: Equivalent Input Force, $d = 0.01$ m

with friction do not necessarily require negative force input because friction is acting in the negative direction of the maneuver. In addition, applying negative pulse may cause velocity reversals in the small velocity region when there is an error in the model parameters for the controller design and/or there is a variation in Coulomb friction. The new bounds on input for this approach are

$$0 \leq u_k \leq u_p \qquad (k = 1, 2, \cdots, N) \tag{20}$$

With the new input bounds, the control input history is shown in Figure 10 with the initial condition and final condition of

$$\underline{x}(0) = \begin{bmatrix} 0 \\ 0 \\ 0 \\ 0 \end{bmatrix} \qquad \underline{x}(t_f) = \begin{bmatrix} 0.001 \\ 0.001 \\ 0 \\ 0 \end{bmatrix} \tag{21}$$

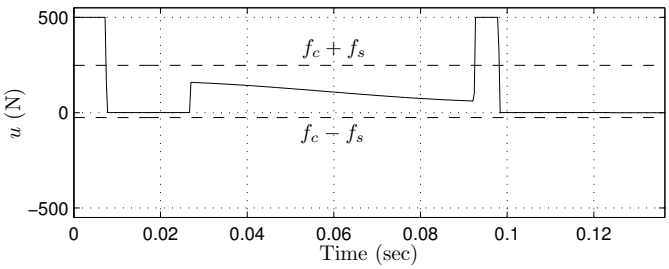

Figure 10: Input Force, displacement 0.001 m

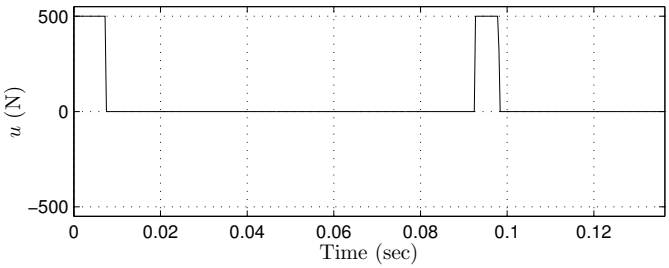

Figure 11: Equivalent Input Force, displacement 0.001 m

After the first pulse in the input profile, the control input is turned off to bring the first mass to a stop and

then starts to compensate Coulomb friction and spring force. However, the controller doesn't need to compensate because the controller profile satisfies Equation 18. Therefore the equivalent control profile becomes two positive pulses with different pulse widths as shown in Figure 11. To verify the equivalent control profile, nonlinear simulation is performed and its response plot is shown in Figure 12.

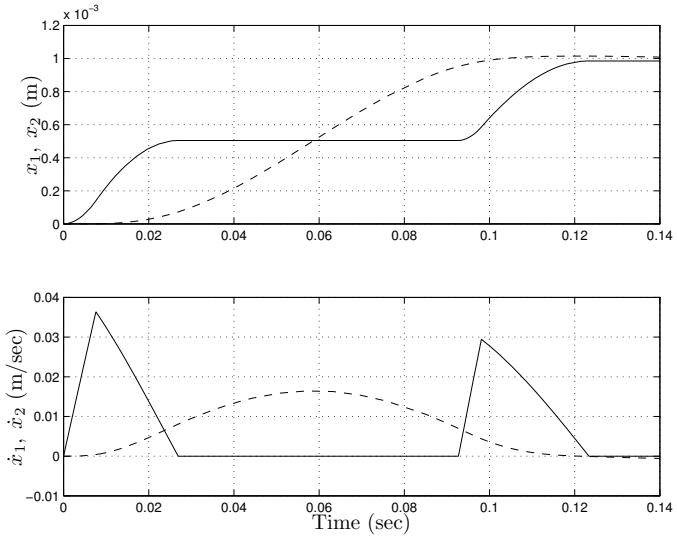

Figure 12: Response from Nonlinear Simulation

The second simulation for positive pulse approach is performed with the initial and final states of

$$\underline{x}(0) = \begin{bmatrix} 0 \\ 0 \\ 0 \\ 0 \end{bmatrix} \qquad \underline{x}(t_f) = \begin{bmatrix} 0.01 \\ 0.01 \\ 0 \\ 0 \end{bmatrix} \tag{22}$$

The input force plot in Figure 13 shows that the compensation of spring force is needed to prevent velocity reversals of the first mass and to stay stuck. The linear simulation responses are shown in 14 and the equivalent input history plot is shown in Figure 15.

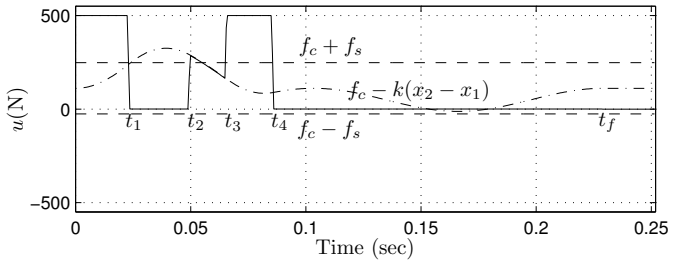

Figure 13: Input Force, displacement 0.01 m

Same approach can be applied for larger displacement, however, there is a large increase in final time, t_f, because the velocity gets larger and available friction force

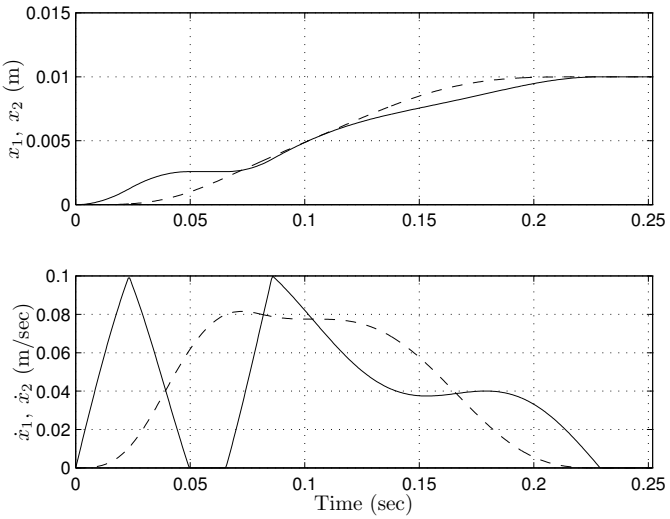

Figure 14: Response Plot, displacement 0.01 m

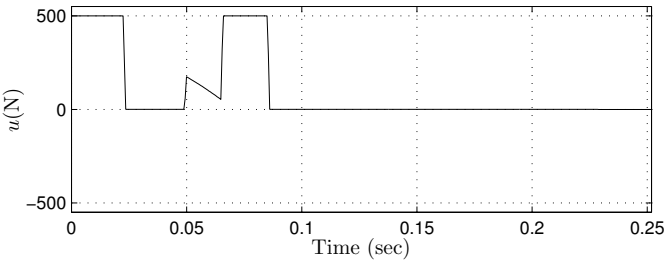

Figure 15: Equivalent Input Force, displacement 0.01 m

is limited. Therefore, two positive pulse solution is more suitable for small displacement or actuating near the reference point. To illustrate this, switching time and final time is given for different displacements in Figure 16. The switching time used in the plot is shown in Figure 13. It is shown that the time between t_4 and t_f becomes larger as displacement becomes bigger. In Figure 16, *Region I* is where the spring force generated during stiction is not large enough to overcome static friction. In this region, two positive pulses are used. In *Region II*, the spring force is compensated to the first mass between t_2 and t_3 to stay stuck. In *Region III*, velocity of the first mass is always positive and the resulting control is a two positive pulse profile.

6 Comparison with Single Pulse Input

It is more convenient to design a controller if the rigid body assumption is made to the flexible body. Yang and Tomizuka [2] developed the pulse width control for a rigid body, and the pulse width for the system is found by the following equation.

$$t_p = \sqrt{\frac{2d(m_1 + m_2)f_c}{f_p(f_p - f_c)}} \tag{23}$$

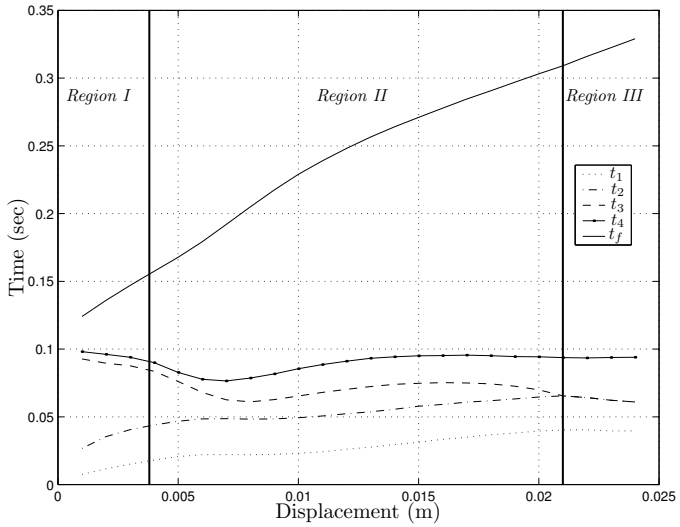

Figure 16: Switching and final time vs. displacement

where, t_p is the pulse width and d is the command displacement. In Figure 17, single pulse input developed in Equation 23 is used to simulate the frictional floating oscillator system. The final time is determined when the first mass comes to rest. It is shown that the final time for the single pulse input in Figure 17 is larger than the final time in Figure 16. Single pulse input will also produce displacement errors and residual vibration of the second mass. In Figure 18, the error of the first mass position and residual energy at the final time is shown for different displacements. Especially when the command displacement is small, the flexible mode of the system will always be excited because of the small pulse width. Therefore, it is necessary to include the flexibility in the controller design for precise positioning systems.

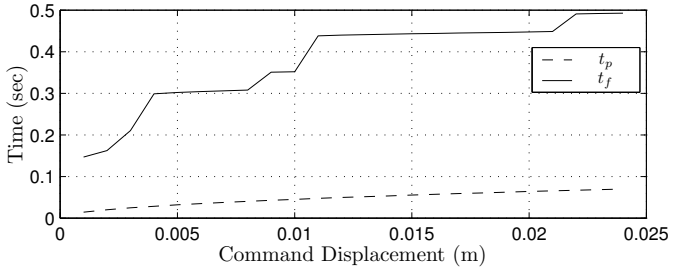

Figure 17: Pulse Width and final time vs. displacement, Single Pulse Input Simulation

7 Conclusion

For a large displacement, bang-bang control with three switches can be found for rest-to-rest maneuvers with friction. The control input resembles the optimal control profile of a linear floating oscillator because they

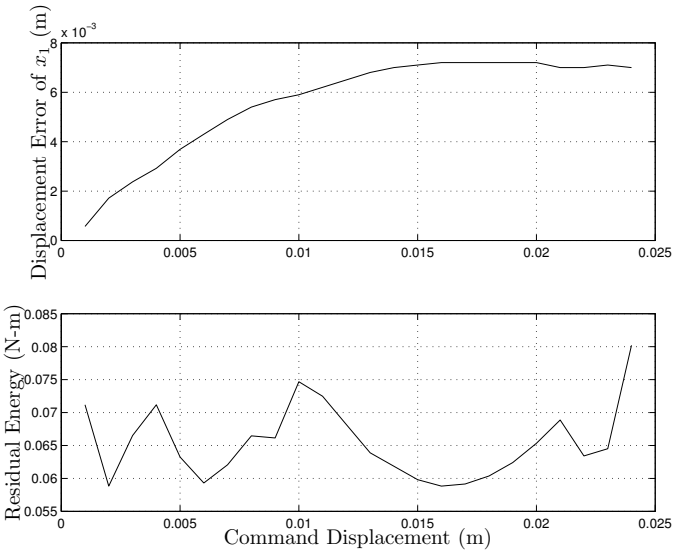

Figure 18: Displacement error and Residual Energy, Single Pulse Input Simulation

have the same number of switches with bang-bang control profile. However, stiction of the first mass occurs when the maneuver displacement is small. In this case, two positive pulse input profile can be used. For systems with an uncertainty in the model parameters and variation in the Coulomb friction, four switch bang-bang control can be used to bring a system near the final states and then positive two pulse control is applied to the final states.

References

[1] Brian Armstrong-Helouvry, Pierre Dupon, and Carlos Canudas De Wit, *A Survey of Models, Analysis Tools and Compensation Methods for the Control of Machines with Friction*, Autometica, Vol. 30, No. 7, pp. 3875-3877, 1994.

[2] Sangsik Yang, and Masayoshi Tomizuka, *Adaptive Pulse Width Control for Precise Positioning Under the Influence of Static and Coulomb Friction*, Journal of Dynamic Systems, Measurement, and Control, Vol. 110, pp 221-227, September 1998.

[3] T. Singh, and S.R. Vadali, *Robust Time Optimal Control: A Frequency Domain Approach*, Journal of Guidance, Control, and Dynamics, Vol. 17, No. 2, Mar-Apr 1994, pp. 346-353.

[4] Brian J. Driessen, *On-Off Minimum-Time Control With Limited Fuel Usage: Near Global Optima Via Linear Programming*, Proceedings of the American Control Conference, Chicago, Illinois, June 2000, pp. 3875-3877.